AIAA 80-1693R

Deployment and Retrieval of Shuttle Supported Tethered Satellites

A.K. Misra*
McGill University, Montreal, Quebec, Canada
and
V.J. Modi†
The University of British Columbia, Vancouver, British Columbia, Canada

The general dynamical model is used to investigate the deployment and retrieval dynamics and control of the tether connected shuttle/subsatellite system. Control of the in-plane motion is provided by letting the difference between the rate of change of the undeformed length of the tether and a commanded length rate vary linearly with the state vector. Successful deployment and retrieval are carried out by judicious selection of commanded length rate and control law gains. It is observed that gains that damp swing oscillations may cause large vibrations. This makes it necessary to simulate the general dynamics in order to evaluate a control strategy.

Nomenclature

$[A],[B],[C],[D]$ = system matrices, Eq. (8)
$[\bar{A}],[\bar{B}],[\bar{C}],[\bar{D}]$ = modified system matrices, Eq. (12)
A_b = area of the subsatellite
A_n, B_n = coefficients of Φ_n in the expression of u and v, respectively ($n=1,2,\ldots$)
c = coefficient describing deployment or retrieval rate
$\bar{c}$ = $c(\times 10^4$ s)
C_d = normal drag coefficient of the tether
C_{db} = normal drag coefficient of the subsatellite
d = diameter of the tether
e = eccentricity of the orbit
h = altitude of any point above the Earth's surface, in meters
h_s = altitude of center of mass of system
h_0 = scale factor in atmospheric model
$H(\theta)$ = function of θ, Eq. (14b)
i = inclination of the orbit to the equatorial plane
$\bar{i},\bar{j},\bar{k}$ = unit vectors along x, y, and z axes, respectively
$[K]$ = gain matrix
L, L_s = undeformed and stretched lengths of the tether, respectively
L_c = command length
L_i, L_f = initial and final unstretched lengths, respectively
m = total mass of the system
m_a, m_b = mass of the end-bodies
m_t = mass per unit length of the tether
q_i = generalized coordinate
Q_i = generalized force
$\bar{Q}_i$ = component of Q_i due to environmental forces
R_0 = radial distance of the center of mass of the tethered system from the center of the Earth
s = coordinate along stretched tether
t = time
T = kinetic energy of the system
u,v = out-of-plane and in-plane transverse vibrations of the tether, respectively
U = potential energy of the system
$\bar{V}$ = velocity of an element of the system relative to air
V_x, V_y, V_z = components of $\bar{V}$ along x, y, and z axes, respectively
x,y,z = a set of coordinate axes fixed to the undeformed tether
α,γ = angles describing the orientation of the tether
α_i = initial value of $\alpha-\pi$
ϵ = axial strain in the tether
$\epsilon_{sh}, \epsilon_{sat}$ = value of ϵ at the shuttle and subsatellite ends, respectively
θ = true anomaly
θ_p = argument of the perigee
$\tilde{\theta}$ = $\theta+\theta_p$
ρ = density of air
ρ_0 = a constant in the exponential model of the density of air
$\rho_b, \rho_s, \tilde{\rho}$ = densities as defined in Eq. (7)
σ = angular velocity of the Earth's atmosphere
Φ_n = nth admissible function
Ω = mean orbital rate

Subscripts and Superscripts

$(\dot{})$ = differentiation with respect to t
$()'$ = differentiation with respect to θ
$()_0$ = reference value of a generalized coordinate

Introduction

RECENTLY, tethered satellite systems have received considerable attention owing to their potential for numerous applications. For example, such a system can be used to carry out sophisticated gravity gradient, ionospheric, or radio astronomy measurements, to deploy payloads into new orbits or retrieve free-flying satellites for servicing, to assist construction of large space platforms, etc. This promising nature of the tethered systems has encouraged several investigators to study their dynamics and control during deployment, stationkeeping, and retrieval stages. The general dynamics of the tethered satellites are rather complex and, naturally, the earlier dynamical models involved a number of oversimplifying assumptions such as planar

Presented as Paper 80-1693 at the AIAA/AAS Astrodynamics Conference, Danvers, Mass., Aug. 11-13, 1980; submitted Sept. 16, 1980; revision received Aug. 17, 1981.

*Assistant Professor, Department of Mechanical Engineering. Member AIAA.
†Professor, Department of Mechanical Engineering. Associate Fellow AIAA.

Table 1 Comparison of dynamical models used in various investigations

	Ebner[1]	Stuiver and Bainum[2]	Rupp[3]	Baker et al.[4]	Kulla[5]	Buckens[6]	Kane and Levinson[7]
Three-dimensional motion	No	No	No	Yes	No	Yes	Yes
Results based on nonlinear analysis	No	...	No	Yes	Yes	No	No
Tether mass	Yes	No	Yes	Yes	Yes	Yes	No
Longitudinal vibration of the tether	No	No	Yes	Yes	No	No	No
Longitudinal strain variation along the tether	No	No	No	No	No	No	No
Transverse vibrations of the tether	Yes	No	Steady state only		Yes	Yes	No
Torsional stiffness of the tether	No	No	No	No	No	No	No
Anisotropy of the tether	No	No	No	No	No	No	No
Discretization procedure	Galerkin	...	...	...	Finite difference	Galerkin	...
Rotational motion of end masses	No	Yes	No	Yes	No	No	No
Offset of the point of attachment at the shuttle	No	Yes	No	No	No	No	No
Aerodynamic drag	No	No	Yes	Yes	Yes	No	No
Rotating atmosphere	No	No	No	Yes	No	No	No

	Kalaghan et al.[8]	Modi and Misra[9]	Modi and Misra[10]	Misra and Modi[11]	Kohler et al.[12]	Bainum and Kumar[13]
Three-dimensional motion	Yes	Yes	Yes	Yes	Yes	Yes
Results based on nonlinear analysis	Yes	No	No	No	Yes	Yes
Tether mass	Yes	Yes	Yes	Yes	Yes	No
Longitudinal vibration of the tether	Masked	Yes	Yes	Yes	Yes	No
Longitudinal strain variation along the tether	Masked	No	No	Yes	Yes	No
Transverse vibrations of the tether	Masked	Yes	Yes	Yes	Yes	No
Torsional stiffness of the tether	No	No	No	No	Yes	No
Anisotropy of the tether	No	No	No	No	Yes	No
Discretization procedure	Point	Galerkin	Galerkin	Galerkin	Finite difference & finite elements	...
Rotational motion of end masses	No	Yes	Yes	Yes	No	No
Offset of the point of attachment at the shuttle	No	No	No	Yes	No	No
Aerodynamic drag	Yes	No	Yes	Yes	Yes	Yes
Rotating atmosphere	Yes	No	Yes	Yes	Yes	Yes

motion, massless tether, point end masses, negligible transverse and longitudinal vibrations, etc. Although recently the models have become more realistic by removing some of these assumptions, the analyses dealing with the control of the system have used comparatively simpler models. A comparison of the models used in various investigations[1-13] is outlined in Table 1.

It is clear from Table 1 that Misra and Modi[11] and Kohler et al.[12] provide the most general dynamical models, although both have some deficiencies. Reference 11 does not consider the torsional rigidity or possible anisotropy of the tether, while Ref. 12 treats the end-bodies as point masses. Furthermore, these two investigations have none or very little control simulation. However, the control of the tethered system during its deployment or retrieval has been considered by some of the other authors. Stuiver and Bainum[2] have studied the planar deployment control of the Tethered Orbiting Interferometer (TOI) satellite, describing an algorithm to find the control forces for a given set of initial and terminal conditions. A tether tension control law for successful deployment and retrieval of the tethered subsatellite system was formulated by Rupp.[3] Although the dynamical model used was very simple (see Table 1), his work is probably the most influential one in the area of tethered satellites. Sub-

sequent analyses[4,5,8] dealing with the deployment, retrieval, and stationkeeping of the tethered systems used a Rupp-type or modified-Rupp-type tension control law. However, the dynamical models and the commanded length histories were different. Recently, Bainum and Kumar[13] developed an optimal control law based on an application of the linear regulator problem. Control was provided by modulating the tension level in the tether as a function of the difference between the actual and commanded tetherline length, length rate, in-plane swing angle, and swing angle rate. This control system turned out to be superior to Rupp-type control; however, the dynamical model used did not include tether vibrations. Spencer,[14] using a simple model, compared the performance of two simple control systems in the presence of atmospheric drag. It was noted that a controller using time varying length commands is superior to one using Rupp- or Kissel-type tension laws for controlling three-dimensional motion of the shuttle/tethered satellite system.

The objective of this paper is to carry out an analysis of the control dynamics using the general formulation outlined in Ref. 11. Instead of using a Rupp-type tension control law, a length rate control law is used, i.e., the rate of unwinding of the tether spool is made to depend on the state variables.

System Description

Consider a system of the space shuttle and a subsatellite having masses m_a and m_b, respectively, and connected by a tether with a mass per unit length m_l (Fig. 1). The instantaneous center of mass S of the system can be located with respect to the center of the Earth E by the radial distance R_0, inclination i of the orbit to the equatorial plane, argument of the perigee θ_p, and true anomaly θ. A and B are the centers of mass of the shuttle and subsatellite, respectively, while P_a and P_b are the points of attachment of the tether having an instantaneous unstretched length L. A set of rotating coordinate axes (x_0, y_0, z_0) are located at S such that the x_0 axis is along the orbit normal, the y_0 axis coincides with the local vertical, and the z_0 axis completes the triad. The coordinate axes x_a, y_a, z_a fixed on the shuttle are obtained from x_0, y_0, z_0 axes through a set of modified Eulerian rotations as follows: β_a about the y_0 axis giving x_a', y_a', z_a'; γ_a about the z_a' axis resulting in x_a'', y_a'', z_a'', and finally α_a about the x_a'' axis yielding x_a, y_a, z_a. The coordinate axes x_b, y_b, z_b fixed to the subsatellite are obtained from x_0, y_0, z_0 axes through a similar set of rotations α_b, β_b, and γ_b. The orientation of the axes x, y, z (y axis coinciding with the nominal tetherline) is defined by only two analogous rotations α and γ, implying an assumption that torsion of the tether about its own axis can be ignored.

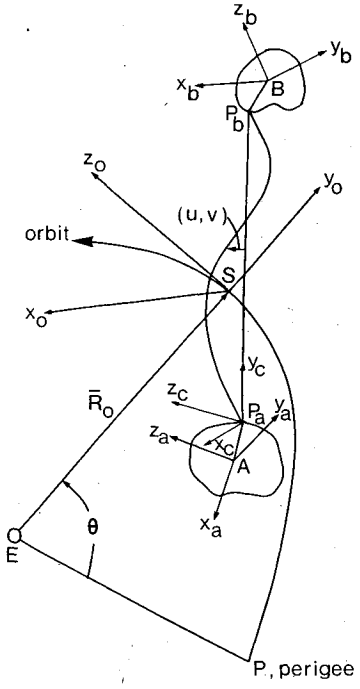

Fig. 1 Geometry of motion.

One must distinguish between the "material coordinate" y along the undeformed tether and "geometrical coordinate" s along the longitudinally deformed tether. The differentials of the two coordinates are related by

$$ds = dy(1+\epsilon) \tag{1a}$$

where ϵ is the axial strain at any instant t in an element dy. In general, ϵ varies along the tether and it is convenient to expand ϵ in a power series

$$\epsilon = \sum_{n=1}^{\infty} \epsilon_n(t) y^{n-1} \tag{1b}$$

This form of expansion is a logical choice, since the axial strain variation is quadratic along a tether aligned with the local vertical in the absence of the environmental effects. It may be noted that truncation of the series to only one term is equivalent to the assumption of uniform strain in the tether. From Eqs. (1a) and (1b),

$$s = \int_0^y dy(1+\epsilon) = y + \sum_{n=1}^{\infty} \epsilon_n \frac{y^n}{n} \tag{1c}$$

and the total stretched length of the tether is

$$L_s = L\left(1 + \sum_{n=1}^{\infty} \epsilon_n \frac{L^{n-1}}{n}\right) \tag{1d}$$

The out-of-plane and in-plane transverse vibrations of the tether, denoted by u and v, respectively, are superposed on the stretched tetherline. For convenience, the transverse vibrations are expanded in terms of a set of admissible functions:

$$u = \sum_{n=1}^{\infty} \phi_n(y) A_n(t) \tag{2a}$$

and

$$v = \sum_{n=1}^{\infty} \phi_n(y) B_n(t) \tag{2b}$$

where

$$\phi_n(y) = \sqrt{2}\sin(n\pi y/L) \tag{2c}$$

Hence the generalized coordinates describing the general motion are α, γ, ϵ_n, A_n, B_n ($n=1,2,\ldots,\infty$) associated with the tether dynamics and α_a, β_a, γ_a, α_b, β_b, γ_b specifying the end-body rotations.

System Equations and Their Linearization

The equations governing the system dynamics can be obtained using the classical Lagrangian formulation

$$\frac{d}{dt}\left(\frac{\partial T}{\partial \dot{q}_i}\right) - \frac{\partial T}{\partial q_i} + \frac{\partial U}{\partial q_i} = Q_i \tag{3}$$

where q_i represents the generalized coordinates and Q_i is the corresponding generalized force arising owing to the environmental and control forces, if any. Here T is the kinetic energy, and U is the sum of the gravitational potential energy and the strain energy associated with transverse and longitudinal deformations. The expressions for T and U are

too lengthy and are omitted here for brevity. They can be found in two previous investigations by the authors (Ref. 9, without strain variation; Ref. 11, with strain variation along the tether). The generalized force Q_i can be split into two parts, $\tilde{Q}_i$ and Q_i^*, owing to the environmental and control forces, respectively. In the present investigation, only one type of environmental force is considered—that due to the atmospheric drag. Other effects, like that of solar radiation pressure, are likely to be much smaller. The aerodynamic force on an element of the system can be expressed as

$$\Delta\bar{F} = -\tfrac{1}{2}C_d\rho(\Delta A)\,\bar{V}|\bar{V}| \tag{4a}$$

where C_d and ρ are the drag coefficient and density of air, respectively, while ΔA is the projected area of the element normal to its velocity $\bar{V}$ relative to the atmosphere. The variation of the density of air is assumed to be exponential, i.e.,

$$\rho = \rho_0 \exp(-h/h_0) \tag{4b}$$

where h is the altitude in meters above the Earth's surface, while ρ_0 and h_0 are two constants. This is an oversimplification of the actual situation, but it is felt that the salient features of the system behavior can be examined with this model.

The relative velocity $\bar{V}$ in Eq. (4a) is the vectorial difference between the orbital velocity of the center of mass of the system and the velocity of the atmosphere due to its rotation about the Earth's axis. The velocity of the element relative to the center of mass of the system resulting from the librations and vibrations is comparatively much smaller and is ignored here. With this approximation, one obtains

$$\begin{aligned}\bar{V} &= V_x\bar{i} + V_y\bar{j} + V_z\bar{k} \equiv [R_0\sigma c\tilde{\theta} s i c\gamma + \dot{R}_0 s\gamma]\bar{i} \\ &+ [-R_0\sigma c\tilde{\theta} s i c\alpha s\gamma + \dot{R}_0 c\alpha c\gamma + R_0(\dot{\theta} - \sigma c i)s\alpha]\bar{j} \\ &+ [R_0\sigma c\tilde{\theta} s i s\alpha s\gamma - \dot{R}_0 s\alpha c\gamma + R_0(\dot{\theta} - \sigma c i)c\alpha]\bar{k}\end{aligned} \tag{5a}$$

where σ is the speed of rotation of the Earth about its axis and

$$\tilde{\theta} = \theta + \theta_p \tag{5b}$$

Substitution of Eqs. (4b) and (5a) into Eq. (4a), application of the principle of virtual work, and some algebraic manipulation yield

$$\tilde{Q}_\alpha = -\tfrac{1}{2}\left[C_d d(V_x^2 + V_z^2)^{1/2}\int_0^L y\rho\,dy + c_{db}\rho_b A_b|\bar{V}|L\right]V_z \tag{6a}$$

$$\tilde{Q}_\gamma = \tfrac{1}{2}\left[C_d d(V_x^2 + V_z^2)^{1/2}\int_0^L y\rho\,dy + c_{db}\rho_b A_b|\bar{V}|L\right]V_x c\alpha \tag{6b}$$

$$\tilde{Q}_{\epsilon n} = -\tfrac{1}{2}\left[C_d d(V_x^2 + V_z^2)^{1/2} \times \int_0^L y^n\rho\,dy + c_{db}\rho_b A_b|\bar{V}|L^n\right]V_y/n \tag{6c}$$

$$\tilde{Q}_{an} = -\tfrac{1}{2}C_d d(V_x^2 + V_z^2)^{1/2}V_x\int_0^L \phi_n\rho\,dy \tag{6d}$$

$$\tilde{Q}_{bn} = -\tfrac{1}{2}C_d d(V_x^2 + V_z^2)^{1/2}V_z\int_0^L \phi_n\rho\,dy \tag{6e}$$

$$(n = 1,2,\ldots,\infty)$$

The expressions for the kinetic and potential energy as well as generalized forces can be introduced into Eq. (3), leading to a set of nonlinear, nonautonomous, and coupled differential equations which are very complex even for computer simulation. Clearly, some simplification must be made. It was decided to linearize the system equations, which usually reduces the complexity considerably without affecting most of the characteristics of the system provided the motions induced can be considered small. In order to carry out linearization one considers small oscillations from a reference state, usually the nontrivial equilibrium. But it is not necessary that the reference state must be the nontrivial equilibrium. Any state can be chosen as a reference state as long as excursions from this state are small. How good the choice of the reference state is can easily be verified by examining the system response data. In the present case, analytical expressions for the nontrivial equilibrium configuration are almost impossible to obtain if one takes into account the eccentricity of the orbit, rotation of the atmosphere, continuously varying length, etc. One can use numerical methods to determine this exact configuration at each time step of the integration scheme; however, it is more convenient to choose a reference state which is simpler to compute but not too far away from the actual nontrivial equilibrium configuration. The steady-state attitude of the nondeploying and nonvibrating system in a circular orbit, arising owing to the aerodynamic drag in a nonrotating atmosphere, can be chosen as such a reference state. Since, in practice, $e \simeq 0.001$, $(\sigma/\Omega) \simeq 0.06$, and the steady-state vibrations are small, the nontrivial equilibrium configuration is quite close to this reference state and any small deviation from the nontrivial equilibrium configuration is also a small deviation from the reference state. With this as background, it may be shown that[10]

$$\gamma_0 = \epsilon_{n0} = A_{n0} = B_{n0} = 0 \tag{7a}$$

and α_0 is the root of the transcendental equation

$$\begin{aligned}&c\alpha_0[3(m_b + m_t L/3)s\alpha_0 \\ &\quad + \tfrac{1}{2}C_d R_0^2\{\tilde{\rho} d|c\alpha_0| + \rho_b A_b/L\}] = 0\end{aligned} \tag{7b}$$

where

$$\tilde{\rho} = \rho_s(h_0/Lc\alpha_0)^2[1 - (1 + Lc\alpha_0/h_0)\exp(-Lc\alpha_0/h_0)] \tag{7c}$$

$$\rho_s = \rho_0\exp(-h_s/h_0) \qquad \rho_b = \rho_s\exp(-Lc\alpha_0/h_0) \tag{7d}$$

and h_s is the altitude of the center of mass of the system.

The variation of α_0 with the length of the tether is shown in Fig. 2 for four different cases. In each case, the shuttle is at the altitude of 220 km (circular orbit) and the subsatellite with a mass of 150 kg has a projected area of 1 m^2. Two materials (stainless steel and kevlar) and two tether diameters (1.0 and 0.5 mm) are considered. Note that the reference state almost coincides with the local vertical for tether lengths up to 50 km. Gradually, the aerodynamic drag becomes large and the tether can deviate as much as 30 deg from the local vertical. For the same diameter, a kevlar tether deviates more than a stainless tether. This large displacement should be kept in mind while assigning the initial conditions during the simulation of retrieval dynamics of the system. Alignment of the tether with the local vertical at the start of the retrieval implies a rather large, not zero, initial displacement from the nontrivial equilibrium configuration.

After linearization around the reference state and change of the independent variable from time t to true anomaly θ, Eq. (3) yields a set of equations which can be put in the form

$$[A]\{q''\} + [B]\{q'\} + [C]\{q\} + \{D\} = \{Q\} \tag{8}$$

where the matrices $[A]$, $[B]$, $[C]$ and vector $\{D\}$ are functions of θ, L, and its derivatives with respect to θ. An examination of the above matrices shows that motion in the

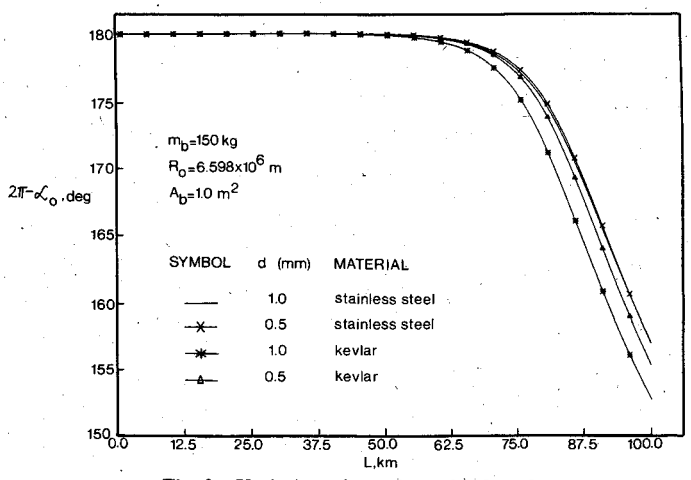

Fig. 2 Variation of α_θ with tether length.

orbital plane and motion perpendicular to the orbital plane are uncoupled. This is in contrast to the nonlinear equations which couple the two types of motion. Linearization enables one to study the two motions separately; however, it involves, naturally, some loss of accuracy.

Control of In-Plane Motion

The in-plane dynamics of the tether system can be controlled by controlling the rotation of the tether feedout spool, thereby controlling L' or the rate of change of the undeformed length of the tether. Hence the control law can be written as

$$L' = L_c' + [K]\{X\} \tag{9}$$

where $\{X\}$ is the vector of the generalized coordinates and velocities describing the in-plane motion; $[K]$ is a gain matrix (row vector); and L_c' is a commanded length rate. This law is an alternative to the tension control law and probably is easier to implement. In order to test the effectiveness of this control, a special case of Eq. (9) is considered, i.e.,

$$L' = L_c' + K_1\alpha + K_2\alpha' = L_c'[1 + \bar{K}_1\alpha + \bar{K}_2\alpha'] \tag{10}$$

where $\bar{K}_1$ and $\bar{K}_2$ are constants. This should damp-out the swing oscillation, which is the most serious component of the in-plane motion.

The quantities L, (L'/L), and (L''/L) appearing in Eq. (8) can easily be calculated from Eq. (10). After linearization, these are

$$L = L_c + \bar{K}_1\Psi + \bar{K}_2\chi \tag{11a}$$

$$L'/L = (L_c'/L_c)\,[1 + \bar{K}_1(\alpha - \Psi/L_c) + \bar{K}_2(\alpha' - \chi/L_c)] \tag{11b}$$

$$L''/L = (L_c''/L_c)\,[1 + -\bar{K}_1(\alpha - \Psi/L_c) + \bar{K}_2(\alpha' - \chi/L_c)] + (L_c'/L_c)\,[\bar{K}_1\alpha' + \bar{K}_2\alpha''] \tag{11c}$$

where

$$\Psi = \int_{\theta_i}^{\theta} \alpha L_c' \mathrm{d}\theta \qquad \chi = \int_{\theta_i}^{\theta} \alpha' L_c' \mathrm{d}\theta \tag{11d}$$

Substitution of Eqs. (10) and (11) into Eq. (8) yields

$$[\bar{A}]\{q''\} + [\bar{B}]\{q'\} + [\bar{C}]\{q\} + \{\bar{D}\} = \{Q\} \tag{12}$$

where $[\bar{A}]$, $[\bar{B}]$, $[\bar{C}]$, and $\{\bar{D}\}$ are functions of true anomaly θ, commanded length L_c and its derivatives, and the gains K_1 and K_2. By choosing L_c, K_1, and K_2 judiciously, deployment and retrieval can be carried out without causing large librational motions.

Deployment

For deployment of the tethered system, commanded length L_c must be an increasing function of time. Various forms of L_c can be used; however, a combination of exponential and uniform deployment appears to be a simple and efficient procedure. In the present investigation, numerical results were obtained by using a commanded length rate as follows:

$$\begin{aligned} \dot{L}_c &= cL_c && (L_i \le L_c \le L_1) \\ &= cL_1 && (L_1 \le L_c \le L_2) \\ &= c(L_1 + L_2 - L_c) && (L_2 \le L_c \le L_f) \end{aligned} \tag{13}$$

where c is a constant. The first and third correspond to the exponential rate, while the second rate is uniform. The commanded length can be written as

$$\begin{aligned} L_c &= L_i \exp[(c/\Omega)\{H(\theta) - H(\theta_i)\}] && (\theta_i \le \theta \le \theta_1) \\ &= L_1[1 + (c/\Omega)\{H(\theta) - H(\theta_1)\}] && (\theta_1 \le \theta \le \theta_2) \\ &= L_2 + L_1 - L_1 \exp[-(c/\Omega)\{H(\theta) - H(\theta_2)\}] && (\theta_2 \le \theta \le \theta_f) \end{aligned} \tag{14a}$$

where

$$H(\theta) = -\tfrac{1}{2}(1-e^2)^{\frac{1}{2}}\left[\frac{2e\sin\theta}{(1+e\cos\theta)} + 2\tan^{-1}\left[\left\{\frac{(1-e)}{(1+e)}\right\}^{\frac{1}{2}}\tan(\theta/2)\right]\right] \tag{14b}$$

Deployment is basically a stable operation as long as the commanded length rate is not very large. Both pitch and vibratory motions are damped; but while the transverse vibrations tend to zero, the pitch displacement from the local vertical approaches a steady-state value of $-2c/3\Omega$. As length increases, the effect of aerodynamic drag becomes predominant and the tether trails the shuttle instead of leading.

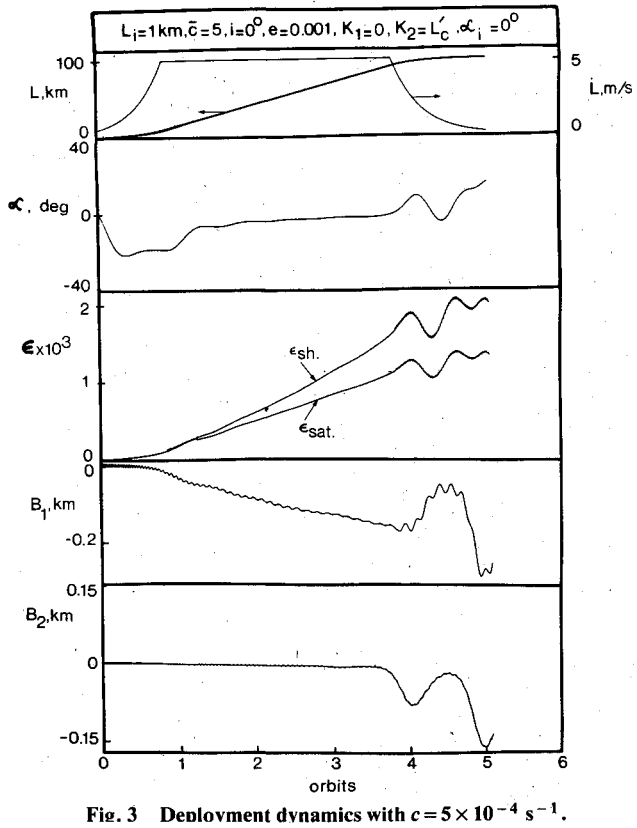

Fig. 3 Deployment dynamics with $c = 5 \times 10^{-4}$ s^{-1}.

All the numerical results presented in this investigation correspond to a 150-kg subsatellite connected to the space shuttle by a tether having a mass density of 1.5 kg/km and a stiffness (Young's modulus $E \times$ area of cross-section A) of 5×10^4 N. The eccentricity of the equatorial orbit is 0.001, while its major axis is 220 km larger than the Earth's radius. Numerical integration of the differential equations was carried out using an International Mathematical and Statistical Library (IMSL) routine based on Gear's method.

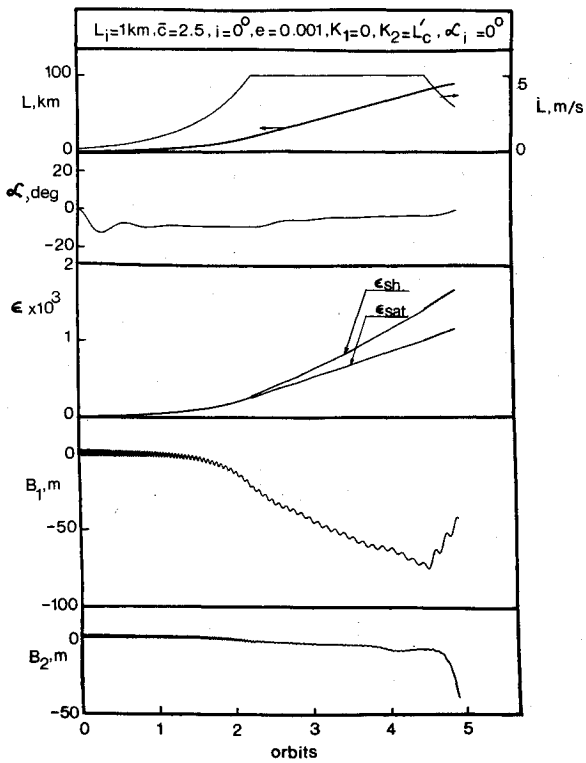

Fig. 4 Deployment dynamics with $c = 2.5 \times 10^{-4}$ s^{-1}.

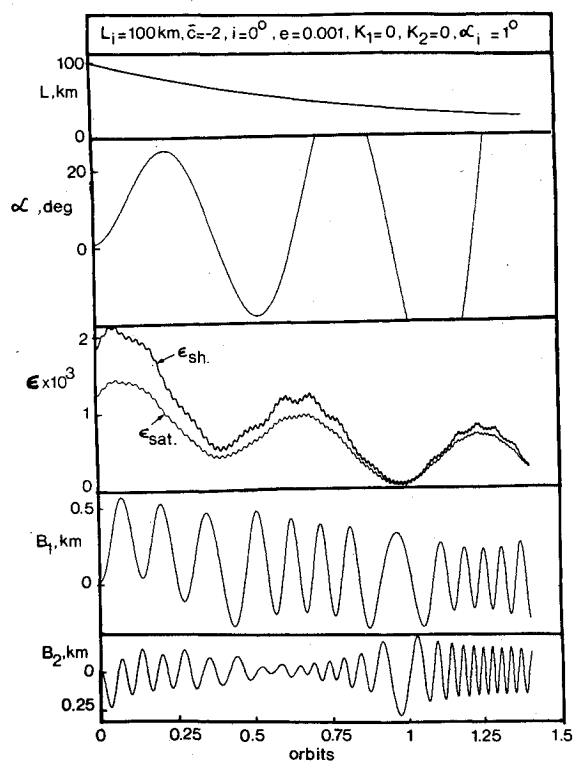

Fig. 5 Uncontrolled retrieval dynamics.

The expansions for longitudinal and transverse vibrations were truncated to three and two terms, respectively. In spite of that, the computing was quite expensive, specially for small lengths. For lengths smaller than 20 km, only one term was retained in the expansion of longitudinal strain.

Figure 3 describes the dynamics during deployment of the tethered system from the initial length of 1 km to the final length of 100 km using $c = 5 \times 10^{-4}$ s^{-1}. The gains K_1 and K_2 are zero and L_c', respectively. It may be noted that the swing angle reaches a numerical maximum of 21 deg after approximately 0.36 orbits; subsequently it reduces in magnitude, changes sign, and oscillates with increasing amplitude owing to increasing aerodynamic drag. The longitudinal strain in the tether at both the shuttle and subsatellite ends increases with length. The vibratory displacements are small until the aerodynamic drag becomes significant.

The deployment dynamics of the same system as above, but with $c = 2.5 \times 10^{-4}$ s^{-1}, are shown in Fig. 4. It may be noted that the maximum swing angle before the aerodynamic effect is felt is much smaller than the previous case (12 deg after 0.30 orbits); however, deployment duration is longer. Once the influence of atmospheric drag becomes large, there is no significant difference in displacements for the two cases. The effects of varying the gains K_1 and K_2 (not shown here) are not that important. The critical part of planning the deployment is the choice of a suitable L_c' or L_c.

Retrieval

Unlike deployment, retrieval of tethered systems is basically an unstable procedure. It involves a negative damping approximately proportional to $\dot{L}/L$. The numerical results presented in this investigation are for exponential retrievals, i.e.,

$$\dot{L}_c = cL_c \qquad (c<0) \tag{15a}$$

Integration and change of independent variable yield

$$L_c = L_i \exp[(c/\Omega)\{H(\theta) - H(\theta_i)\}] \tag{15b}$$

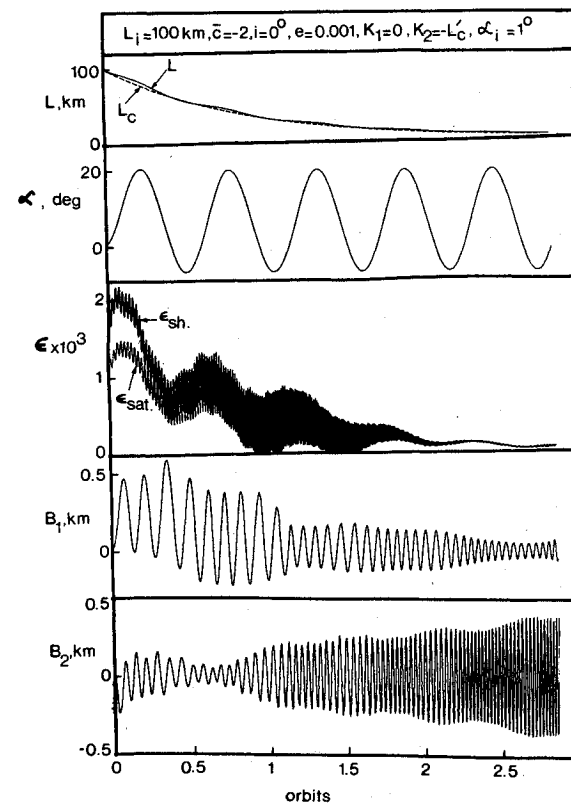

Fig. 6 Controlled retrieval dynamics: $K_1 = 0$, $K_2 = -L_c'$, $\alpha_i = 1$ deg.

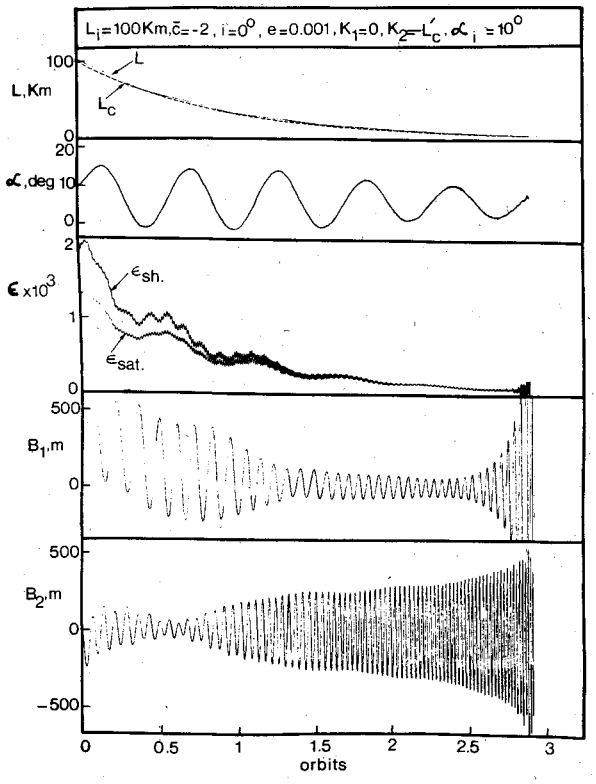

Fig. 7 Controlled retrieval dynamics: $K_1 = 0, K_2 = -L_c', \alpha_i = 10$ deg.

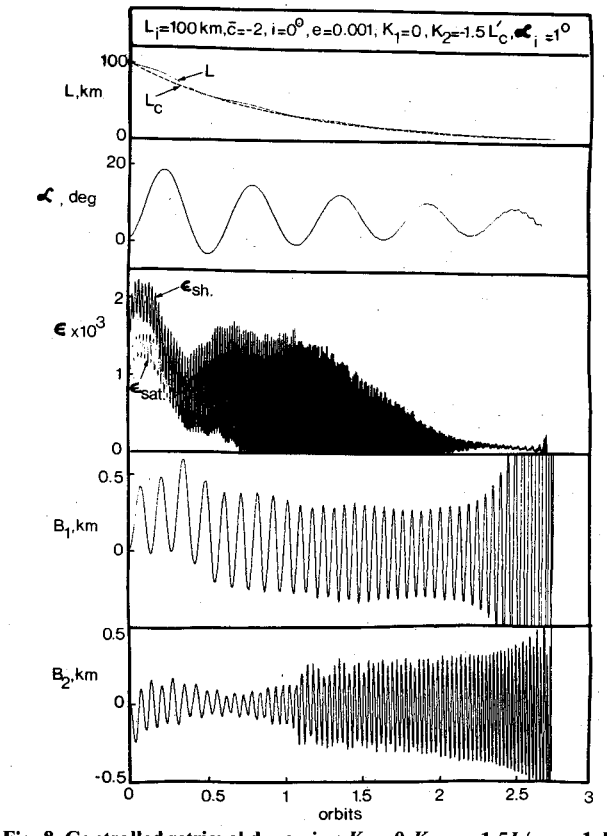

Fig. 8 Controlled retrieval dynamics: $K_1 = 0, K_2 = -1.5L_c', \alpha_i = 1$ deg.

The dynamics during retrieval of the tethered subsatellite system described above are represented by Figs. 5-8. The initial length and c are 100 km and -2×10^{-4} s^{-1}, respectively. In Figs. 5, 6, and 8, the initial pitch displacement is 1 deg from the local vertical, while in Fig. 7 it is 10 deg. Initial vibratory displacements for all the cases are $B_1 = 20$ m, $B_2 = 10$ m, $\epsilon_1 = 1.8734 \times 10^{-3}$, $\epsilon_2 = 0$, and $\epsilon_3 = -0.6245 \times 10^{-4}$. (The initial longitudinal strains correspond to the equilibrium values in the absence of any environmental effects.)

Figure 5 shows the uncontrolled (i.e., $K_1 = K_2 = 0$) retrieval dynamics of the system. One may note the strong growth of swing oscillations. Numerical integration was terminated when the displacements became so large as to make the linear analysis meaningless. Controlled retrieval of the system with $K_1 = 0$ and $K_2 = -L_c'$ is shown in Fig. 6. It may be pointed out that the time scale is different from that in Fig. 5. The librational motion and the longitudinal vibrations are bounded now; but B_2 appears to be growing slowly! As the high frequency longitudinal vibrations make the computation very expensive for small tether lengths, numerical integration has been carried out only up to 5 km; however, the trend is likely to continue for smaller lengths. The transverse vibration represented by B_2 can be damped only by taking appropriate nonzero gains in Eq. (9) associated with transverse vibrations; but what is more important is to note that a general model must be used to evaluate a control strategy adequately. Retrieval dynamics represented in Fig. 7 correspond to the same gain as in Fig. 6; however, initially the swing displacement is 10 deg behind the local vertical. This is a less severe initial condition and hence the pitch oscillations are smaller. Figure 8 represents retrieval with $K_1 = 0$ and $K_2 = -1.5\,L_c'$. Note that although the pitch oscillations are gradually decaying, the transverse and longitudinal vibrations are building up. It appears that K_2 should be in the neighborhood of $-L_c'$ for best results.

Control of Out-of-Plane Motion

Controlling the length rate has no effect on the out-of-plane motion if the system equations are linearized. The same is true for the linear system controlled by a tether tension law. However, both changes in length rate and tension have second-order coupling with the out-of-plane motion, and three-dimensional control can be carried out by using tension or length rate control law provided one uses the nonlinear equations.

As noted earlier, the study of the complete set of nonlinear equations is very complex. Hence to start with, nonlinear librational equations in the absence of vibrational displacements can be studied using the control law outlined in Eq. (9). Since the librations cause the maximum problems, a reasonable insight to the problem can be obtained from this investigation. Subsequently, efforts will be made to simulate the complete set of nonlinear equations. At present, a study of the out-of-plane motion is in progress.

Concluding Remarks

The salient features characterizing the investigation may be summarized as follows:

1) The in-plane control of the deployment/retrieval dynamics of tethered subsatellite systems is studied using a general formulation.

2) The study is based on a length rate control law.

3) The control gains are not that critical for deployment; however, for retrieval, they must be chosen very carefully. Gains that damp-out swing oscillations may cause large vibrational displacements. Hence the general dynamics must be simulated to evaluate a control strategy.

4) Nonlinear equations must be used to simulate the three-dimensional motion if the length rate control law is used.

5) The results presented here should prove useful in selecting a suitable control system for the shuttle supported tethered subsatellite system.

Acknowledgments

The investigation reported here was supported by the Natural Sciences and Engineering Research Council of Canada, Grants A-0967 and A-2181. The help provided by our research assistant, Mr. T.T. Pham, is greatly appreciated.

References

[1]Ebner, S.G., "Deployment of Rotating Cable-Connected Space Stations," *Journal of Spacecraft and Rockets,* Vol. 7, Oct. 1970, pp. 1274-1275.

[2]Stuiver, W. and Bainum, P.M., "A Study of Planar Deployment Control and Libration Damping of a Tethered Orbiting Interferometer Satellite," *The Journal of the Astronautical Sciences,* Vol. 20, May-June 1973, pp. 321-346.

[3]Rupp, C.C., "A Tether Tension Control Law for Tethered Subsatellites Deployed Along Local Vertical," NASA TMX-64963, Sept. 1975.

[4]Baker, W.P. et al., "Tethered Subsatellite Study," NASA TMX-73314, March 1976.

[5]Kulla, P., "Dynamics of Tethered Satellites," *Proceedings of the Symposium on Dynamics and Control of Non-Rigid Spacecraft,* Frascati, Italy, May 1976, pp. 349-354.

[6]Buckens, F., "On the Motion Stability of Tethered Satellite Configurations," *Proceedings of the 12th International Symposium on Space Technology and Science,* edited by H. Nagasu, AGNE Publishing Inc., Tokyo, 1977, pp. 351-358.

[7]Kane, T.R. and Levinson, D.A., "Deployment of a Cable-Supported Payload from an Orbiting Spacecraft," *Journal of Spacecraft and Rockets,* Vol. 14, July 1977, pp. 409-413.

[8]Kalaghan, P.N., Arnold, D.A., Colombo, G., Grassi, M.D., Kirschner, L.R., and Orringer, O., "Study of the Dynamics of a Tethered Satellite System (Skyhook)," Final Rept. Contract NAS8-32199, Smithsonian Institution, Astrophysical Observatory, Cambridge, Mass., March 1978.

[9]Modi, V.J. and Misra, A.K., "Deployment Dynamics of a Tethreed Satellite System," AIAA Paper 78-1398, Aug. 1978.

[10]Modi, V.J. and Misra, A.K., "On the Deployment Dynamics of Tether Connected Two-Body Systems," *Acta Astronautica,* Vol. 6, 9, 1979, pp. 1183-1197.

[11]Misra, A.K. and Modi, V.J., "A General Dynamical Model for the Space Shuttle Based Tethered Subsatellite System," *Advances in the Astronautical Sciences,* Vol. 40, Part II, 1979, pp. 537-557.

[12]Kohler, P., Maag, W., Wehrli, R., Weber, R., and Brauchli, H., "Dynamics of a System of Two Satellites Connected by a Deployable and Extensible Tether of Finite Mass," Contract Rept., ESTEC Contract 2992/76/NL/AK(SC), Vols. 1 and 2, Oct. 1978.

[13]Bainum, P.M. and Kumar, V.K., "Optimal Control of the Shuttle-Tethered-Subsatellite System," Paper 79-190, presented at the 30th Congress of the International Astronautical Federation, Munich, FRG, Sept. 1979.

[14]Spencer, T.M., "Atmospheric Perturbation and Control of a Shuttle/Tethered Satellite," Paper 79-165, presented at the 8th IFAC Space Symposium, Oxford, U.K., July 1979.